

## Pressure-induced ferro- to antiferromagnetic transition in a purely organic compound, $\beta$ -phase *para*-nitrophenyl nitronyl nitroxide

Masaki Mito and Tatsuya Kawae

*Department of Applied Science, Faculty of Engineering, Kyushu University, Fukuoka 812-81, Japan*

Masaharu Takumi and Kiyofumi Nagata

*Department of Applied Physics, Faculty of Science, Fukuoka University, Fukuoka 814-80, Japan*

Masafumi Tamura

*Department of Physics, Faculty of Science, Toho University, Funabashi, Chiba 274, Japan*

Minoru Kinoshita

*Department of Materials Science, Faculty of Science and Engineering, Science University of Tokyo at Yamaguchi, Onoda, Yamaguchi 756, Japan*

Kazuyoshi Takeda

*Department of Applied Science, Faculty of Engineering, Kyushu University, Fukuoka 812-80, Japan*

(Received 19 June 1997)

A pressure-induced ferro- to antiferromagnetic transition in genuine organic compounds has been observed in the  $\beta$ -phase *para*-nitrophenyl nitronyl nitroxide crystal. The transition temperature  $T_C(p)$  in the ferromagnetic state decreases as  $T_C(p) = T_C(p_0)(1 + ap)$  for pressures  $p \leq p_c = 6.5 \pm 0.5$  kbar [ $T_C(p_0) = 0.61$  K,  $a = -0.048$  (kbar $^{-1}$ )]. For  $p > p_c$ , however, experiment demonstrates intrinsically the existence of an antiferromagnetic state as well as a pressure-induced enhancement of  $T_C(p)$  with  $a = 0.004$  (kbar $^{-1}$ ). The results are discussed within the context of theories derived from the unrestricted Hartree-Fock approximation. [S0163-1829(97)51246-X]

The realization of bulk ferromagnetism in genuine organic substances consisting exclusively of light elements such as H, C, N, and O has long been one of the major subjects in the field of material science. There have been mainly two guiding strategies for this; one is to elevate spin multiplicity within polymers by intramolecular or ‘‘through-bond’’ interactions.<sup>1</sup> A variety of investigation by this means have been reported so far.<sup>2</sup> The other is to bring about ferromagnetic interaction between stacked radical molecules by ‘‘through-space’’ exchange interactions. This originates in the so-called McConnell strategy<sup>3</sup> where the interaction between A and B molecules is described by Eq. (1) as

$$H^{AB} = - \sum_{ij} J_{ij}^{AB} S_i^A S_j^B = - S^A S^B \sum_{ij} J_{ij}^{AB} \rho_i^A \rho_j^B. \quad (1)$$

Here  $J_{ij}^{AB}$ ,  $S_i^A(S_j^B)$ ,  $\rho_i^A(\rho_j^B)$  and  $S^A(S^B)$  are exchange integral between atomic-site  $i$  and  $j$  on the two molecules,  $\pi$ -electron spin operator on the site  $i(j)$  of A(B) molecule, spin density on the site  $i(j)$  and the total spin operator for molecule A(B), respectively. One of the experimental checks of the spin density notation [Eq. (1)] is examined on the carbene dimers, for example.<sup>4</sup> However, most radical molecules crystallize antiferromagnetically except in quite a limited case such as galvinoxyl. Through the investigation of this exceptional case, the ferromagnetic interaction is revealed to originate mostly in the indirect charge transfer between the unpaired electrons on each molecule via fully occupied molecular orbitals (MO's) and/or unoccupied MO's, not by di-

rect charge transfer between singly occupied MO's (SOMO's).<sup>5</sup> Extending this strategy to various radical derivatives, one of the present authors [M.K.] and his group eventually succeeded in synthesizing a genuine organic ferromagnet,  $\beta$ -phase *para*-nitrophenyl nitronyl nitroxide ( $\beta$ -*p*-NPNN;  $C_{13}H_{16}N_3O_4$ , Fig. 1) which orders three dimensionally at  $T_C = 0.6$  K.<sup>6-8</sup> Up to now, more than ten radical crystals have been reported to be ferromagnetic, including N,N'-dioxy-1,3,5,7-tetramethyl-2,6,-diazadamantane ( $T_C = 1.48$  K).<sup>9</sup>

Compared with  $d$  or  $f$  electrons in insulating inorganic compounds, the unpaired electrons in organic radicals delocalize rather widely on the molecules. With the help of advanced technique for topological analysis of crystal structures, the recent development of MO calculation gives reliable estimation of spin and charge densities on each constituent atomic site in the molecule on the basis of the unrestricted Hartree-Fock (different orbitals for different spins) approximations, as well as energy levels of each MO. The contribution of MO's to the magnetic interactions has been detailed in the charge transfer mechanism<sup>5,8</sup> or in the *ab-initio* methods,<sup>10,11</sup> as effectively described as the isotropic Heisenberg Hamiltonian,

$$H^{AB} = - J^{AB} S^A S^B, \quad (2)$$

which awaits checks from the experimental side. Here we comment that the anisotropic exchange term (such as  $J_{xy}$ ) is

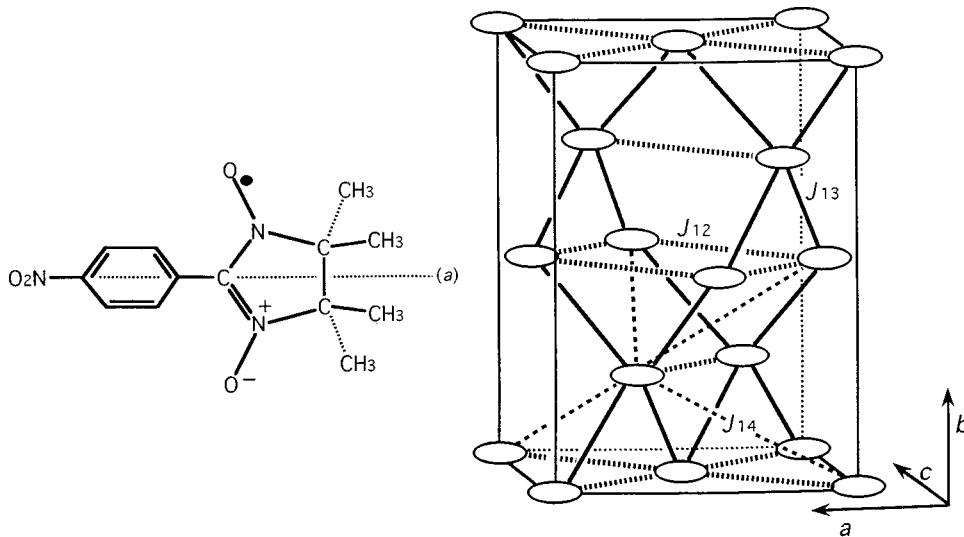


FIG. 1. Schematic molecular structure of *p*-NPNN and the elongated diamond structure of the crystallized  $\beta$  phase. The molecular axis (*a*) is along the *a* axis of the crystal structure, where each ellipse stands for the *p*-NPNN molecule.  $J_{12}$ ,  $J_{13}$ , and  $J_{14}$  indicate the dominant exchange interactions among adjacent molecules.

weak in organic systems where the quenching of angular momentum of molecular orbitals is almost complete.

In this paper, we give experimental demonstrations of the pressure-induced ferro- to antiferromagnetic transition in genuine organic compounds with  $\beta$ -*p*-NPNN, following our previous finding of the pressure-induced reduction of the Curie temperature, and of magnetic dimensionality in the region  $p \leq 7.7$  kbar.<sup>12</sup> Magnetic<sup>6,7</sup> and structural<sup>13</sup> properties of  $\beta$ -*p*-NPNN are studied in detail by various experimental methods.<sup>8</sup> These experimental findings, together with the pressure dependence of lattice parameters observed here at room temperature, are discussed on the recent theoretical background of the intermolecular magnetic interactions. We remark here that the reproducibility of the present results is ascertained for the cycling of pressurization between ambient and nonzero pressures.

Figure 2 shows the pressure dependence of the ac-susceptibility  $\chi_{ac}$  for the polycrystalline  $\beta$ -*p*-NPNN (72.2

mg) up to  $p = 10.4$  kbar, which is taken with the CuBe pressure clamp cell<sup>12</sup> under the ac-field  $H_{ac}(\nu) < 1$  Oe, with frequency  $\nu = 15.9$  Hz. The results at the ambient pressure  $p_0$  are quite the same as those reported for the temperature region above 0.4 K.<sup>7</sup> It is known that the Curie temperature  $T_C(p)$  determined from the crossing point of the extrapolated straight lines from above and below  $T_C$ , as in Fig. 2, agrees with  $T_C$  determined by the heat capacity measurement for  $p \leq 7.7$  kbar.<sup>12</sup> From Fig. 2, we see some remarkable points as follows. The value of  $\chi_{ac}$  in the ordered state decreases sensitively to the increasing pressure: The shoulderlike curve of  $\chi_{ac}$  around  $T_C(p)$  changes into a cusp for  $p > 6$  kbar, giving only a trace at  $p = 10.4$  kbar, where  $\chi_{ac}$  is slightly larger than that in the paramagnetic state around 1 K. It is demonstrated that  $T_C(p)$ , which initially decreased with increasing pressure up to  $p \approx 6$  kbar as  $T_C(p) = T_C(p_0)(1 + ap)$  with  $a = -0.048$  (kbar<sup>-1</sup>), flinches at  $p_c = 6.5 \pm 0.5$  kbar and turns to increase with a small but positive value of  $a = 0.004$  (kbar<sup>-1</sup>) for  $p > 7$  kbar, just as the pressure-induced enhancement of the Néel temperature of organic antiferromagnets referred to in Ref. 12. These results indicate that the ferromagnetic phase changes into some antiferromagnetic phase around  $p_c$ . (The small plateau around 1 K in Fig. 2 is due to the signal from Al metal for the pressure calibration at low temperatures.)

Figure 3 illustrates the characteristic magnetization curves of the polycrystalline  $\beta$ -*p*-NPNN under various pressures, which are obtained at a fixed temperature below  $T_C$  by the integration of  $\chi_{ac}(H)$  against the external field  $H$ . Since  $\chi_{ac}(H)$  did not exhibit any relaxation effect for the ac-field  $H_{ac}(\nu) < 1$  Oe with  $\nu = 15.9$  Hz,  $\chi_{ac}(H)$ , which is observed here, practically corresponds to the differential susceptibility  $dM/dH$ . The values of  $\chi_{ac}$  observed even with 123 Hz (Ref. 7) and 200 Hz (Ref. 12) for this sample do not give any relaxation effect either. The magnetization ( $M$ ) at  $p = 1.2$  kbar (0.34 K) shows essentially the same ferromagnetic behavior at ambient pressure at  $T = 0.44$  K,<sup>7</sup> although the limited field range  $|H| \leq 200$  Oe is given here for the following significant change in this narrow range. The rapid growth of  $M$  at  $p = 1.2$  kbar becomes gradual against the increase of external field  $H$  for the higher pressures. It is

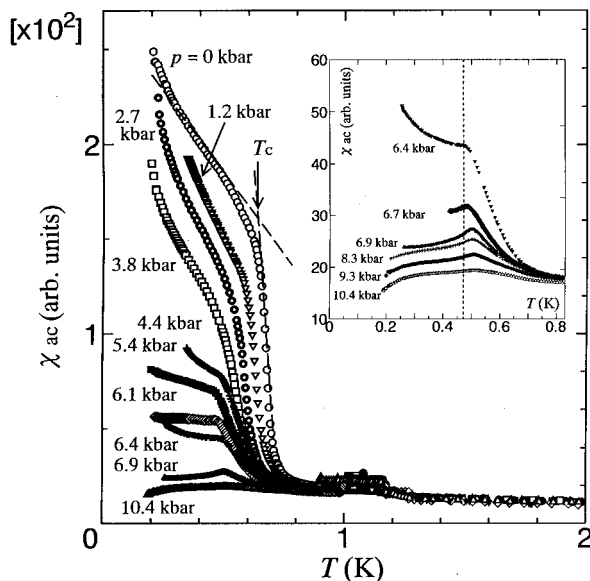


FIG. 2. Pressure dependence of the ac-magnetic susceptibility of  $\beta$ -*p*-NPNN up to 10.4 kbar around the transition temperature.

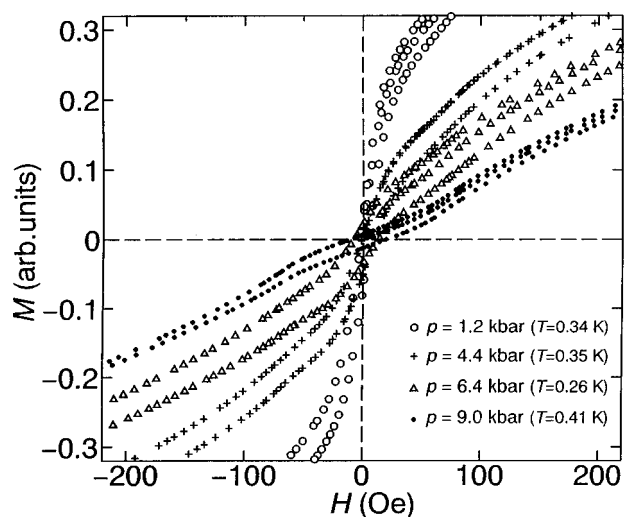


FIG. 3. Magnetization of  $\beta$ - $p$ -NPNN against the external field  $H$ .

noteworthy that the  $M$ - $H$  curve at  $p=9.0$  kbar draws qualitatively different from that in the ferromagnetic state: Rather it looks like an  $M$ - $H$  curve characteristic of an antiferromagnetic with a spin flopping field of some  $H_{\text{fl}} \approx 50$  Oe. A small hysteresis is seen even for  $p=9.0$  kbar, which may be due to canted-weak ferromagnetic moments accompanied in this phase. Even in the Heisenberg organic antiferromagnets with a small anisotropy in the  $g$ -factor ( $\Delta g/g=0.3\%$ ), the weak ferromagnetic moments are probable as in a verdazyl radical crystal and others.<sup>14</sup> These may become much clearer if we can observe the  $M$ - $H$  curve with a single crystal at low temperature.

Other experimental demonstration for the antiferromagnetic behavior for  $p > p_C$  is seen in Fig. 4, which shows the temperature dependence of  $\chi_{\text{ac}}(H)$  measured at various applied field strengths. The cusp of  $\chi_{\text{ac}}(H)$  clearly shifts down to the lower temperatures by the application of the external field. The inset of the figure shows the relation between the applied field and  $T_C(p)$  as determined from the cusp.  $T_C(p)$

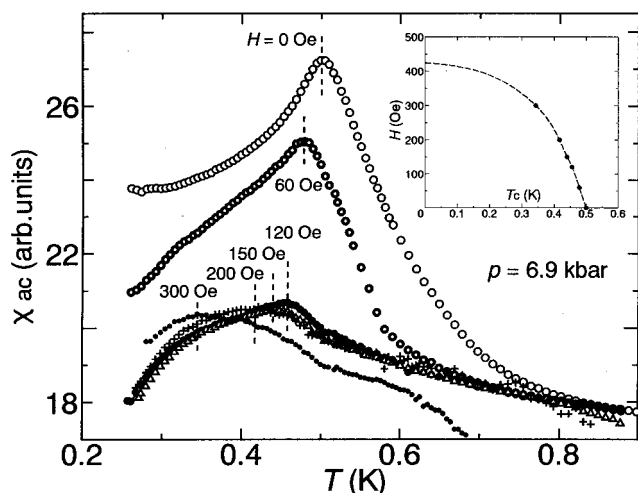


FIG. 4. Field dependence of the ac susceptibility of  $\beta$ - $p$ -NPNN at  $p=6.9$  kbar. The inset shows the  $T_C$ - $H$  phase boundary.

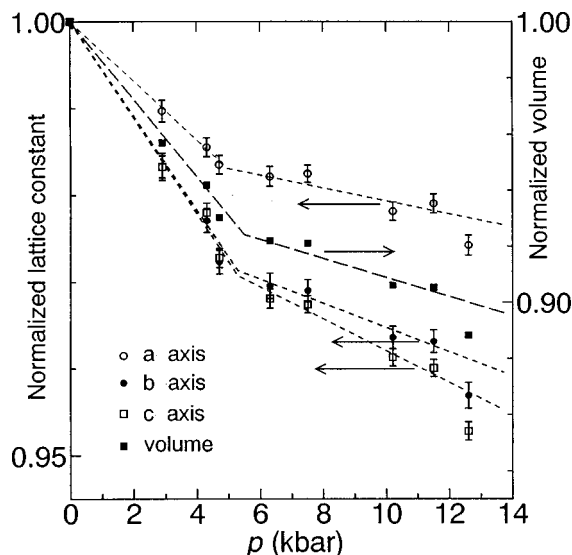


FIG. 5. Pressure dependences of the lattice parameters of  $\beta$ - $p$ -NPNN up to 12.6 kbar normalized to those at ambient pressure.

decreases with the increase of  $H$ . This behavior is characteristic of an antiferromagnet. A similar phenomenon has been observed and theoretically analyzed in the case of antiferromagnetic  $\gamma$ -phase  $p$ -NPNN.<sup>7</sup> However, the pressure-induced antiferromagnetic state of  $\beta$ - $p$ -NPNN is different from that of the  $\gamma$ -phase  $p$ -NPNN, which has a much stronger interaction ( $2J/k_B=4.3$  K) than any interaction in  $\beta$ - $p$ -NPNN as is mentioned below.

The pressure dependence of the lattice parameters of  $\beta$ - $p$ -NPNN up to  $p=12.6$  kbar at room temperature is shown in Fig. 5. The crystal of  $\beta$ - $p$ -NPNN belongs to the space group of  $F2dd$  with  $a=12.374$  Å,  $b=19.350$  Å, and  $c=10.960$  Å at ambient pressure.<sup>13</sup> The rapid x-ray analysis with an imaging plate and a diamond anvil cell is utilized here.<sup>15</sup> The  $R$  factor of this crystallographic analysis is  $R_{\text{WP}}=4.9-10.59\%$  ( $S=5.7-12.3$ ). The diffraction pattern is nearly identical at various pressures, but shifts to the direction of the wide angle with increasing pressure. This indicates that the crystal shrinks while maintaining crystal symmetry at the highest pressure applied here. Each lattice constant, estimated by the Rietvelt method, seems to shrink in two ways depending on the pressure range  $p \geq 5$  kbar, as well as the unit cell volume. The ratio of the shrinkage, which amounts to at most 4.5% along the  $c$  axis, exceeds the largest thermal shrinkage of 2.1% along the  $c$  axis from 300 to 6 K.<sup>16</sup>

The experimental results mentioned so far cannot be explained with the spin density product notation Eq. (1) as it is. When we write the effective interaction between A and B molecules as in Eq. (2),  $J^{\text{AB}}$  contains the kinetic ( $J_K^{\text{AB}}$ ) and the potential ( $J_P^{\text{AB}}$ ) terms as

$$J^{\text{AB}} = J_K^{\text{AB}} + J_P^{\text{AB}}. \quad (3)$$

Both of them depend on the overlap of MO's between A and B molecules in real space, where each MO is constructed on the basis of the unrestricted Hartree-Fock (different orbitals for different spins) approximation. What is stressed in the

ferromagnetic interaction of the galvinoxyl radical crystal is the importance of the charge transfer mechanism relevant to  $J_{\mathbf{K}}^{\text{AB}}$ ,

$$J_{\mathbf{K}}^{\text{AB}} = -\frac{t_{\text{SS}}^2}{U} + \frac{t_{\text{SF}}^2}{U^2} J^{\text{in}} + (\text{terms related to other paths}), \quad (4)$$

where  $t_{\text{SS}}$  stands for the transfer integral between SOMO's of A and B molecules,  $t_{\text{SF}}$  for that between SOMO and other fully occupied MO,  $U$  is the on-site Coulomb repulsion, and  $J^{\text{in}}$  is the intramolecular exchange integrals. Then interplay or frustration among these contributions may result in  $J^{\text{AB}} = 0$  in a certain condition, giving  $T_{\text{C}}(p) = 0$  K. In the case of  $\beta$ -*p*-NPNN, however, we have to take at least twelve molecules adjacent to a central molecule in its diamondlike structure as schematically drawn in Fig. 1. The corresponding exchange integrals are classified into three groups from the symmetry of the crystal structure with respective value  $J_{12}$ ,  $J_{13}$ , and  $J_{14}$ . From the heat capacity measurement at 7.2 kbar,<sup>12</sup> the pressure-induced reduction of the magnetic dimensionality from the three- to two-dimensional Heisenberg system is pointed out from the appearance of short-range order effect by the heat capacity measurements. With the present notation  $J_{12}$ ,  $J_{13}$ , and  $J_{14}$ , the transition temperature  $T_{3\text{d}}$  in such a reduced system can be written as

$$k_{\text{B}}T_{3\text{d}} \propto S^2 \xi_{2\text{d}}^2 (J_{12}, T_{3\text{d}}) \{|J_{13} + J_{14}|\}, \quad (5)$$

from the mean field theory, where  $\xi_{2\text{d}}$  is the spin correlation length in the ac plane in which  $J_{12} \approx 0.8$  K is estimated at  $p = 7.2$  kbar.<sup>12</sup> The antiferromagnetic behavior, we have found here, is taken to originate with the inversion of the sign of interlayer exchange interaction  $J_{13}$  according to Eq. (4) under the pressure. Another interlayer interaction  $J_{14}$ , pointed out to have initially a negative sign as mentioned below, must also remain antiferromagnetic under the pressure to explain the present experimental results. The spin flopping field of the order 50 Oe is relevant to the magnitude

of  $J_{13}$  and  $J_{14}$ , as well as the anisotropy, probably due to the dipole-dipole interaction.<sup>12</sup>

By the *ab initio* theoretical study,  $J_{12}$  is dominantly ferromagnetic ( $0.18 \text{ cm}^{-1}$ ),  $J_{13}$  is secondary ( $0.07 \text{ cm}^{-1}$ ), and  $J_{14}$  is antiferromagnetic ( $-0.014 \text{ cm}^{-1}$ ) at ambient pressure.<sup>10,11</sup> From Fig. 5, the shrinkage of intermolecular distance for  $J_{12}$  is expected to be less than 2% around  $p \approx p_{\text{C}}$ . It is difficult for  $J_{12}$  to reduce its value so much to change its sign. Our previous work indicates  $J_{12} \approx 0.8$  K ( $> 0$ ) at 7.2 kbar.<sup>12</sup> Recent calculation by Yamaguchi *et al.* suggests a possibility of the inversion of the sign of  $J_{13}$  for a few percent of the shrinkage along the *c* axis.<sup>17</sup> With a single crystal of  $\beta$ -*p*-NPNN, we are trying to get clearer results including the structural analysis under pressure.

In summary, we have found a ferro- to antiferromagnetic transition in genuine organic radical compounds, with the pressurized  $\beta$ -*p*-NPNN, through the experiments of the magnetic susceptibility in the external field, (*M-H*) magnetization, as well as the pressure dependence of the lattice constants at room temperature. The transition temperature  $T_{\text{C}}(p)$  in the ferromagnetic state, which has the initial value  $T_{\text{C}}(p_0) = 0.61$  K at ambient pressure  $p_0$ , decreases as  $T_{\text{C}}(p) = T_{\text{C}}(p_0)(1 + ap)$  for  $p < p_{\text{C}} = 6.5 \pm 0.5$  kbar with  $a = -0.048$  ( $\text{kbar}^{-1}$ ). For  $p > p_{\text{C}}$ , however, experiment demonstrates intrinsically the existence of an antiferromagnetic state, in such a *M-H* magnetization curve involving the spin-flopping behavior, as well as the pressure-induced enhancement of  $T_{\text{C}}(p)$  with a positive value of  $a = 0.004$  ( $\text{kbar}^{-1}$ ). The results are understood by the pressure effects which change the intermolecular interlayer interaction  $J_{13}$  from ferro- to antiferromagnetic and also strengthen the interlayer antiferromagnetic  $J_{14}$ , leaving the dominant intralayer  $J_{12}$  ferromagnetic. These are discussed in comparison with the recent theoretical works for magnetic interactions by the charge transfer mechanism and *ab initio* calculation of molecular orbitals on the unrestricted Hartree-Fock approximation.

<sup>1</sup>N. Mataga, *Theor. Chim. Acta* **10**, 372 (1968); A. A. Ovchinnikov, *ibid.* **47**, 297 (1978).

<sup>2</sup>See, for example, D. A. Kaisaki, W. Chang, and D. A. D. Dougherty, *J. Am. Chem. Soc.* **113**, 2764 (1991); M. Matsushita, T. Nakamura, T. Momose, T. Shida, Y. Teki, T. Takui, T. Kinoshita, and K. Itoh, *ibid.* **114**, 7470 (1992).

<sup>3</sup>H. M. McConnell, *J. Chem. Phys.* **39**, 1910 (1963).

<sup>4</sup>A. Izuoka, S. Murata, T. Sugawara, and H. Iwamura, *J. Am. Chem. Soc.* **107**, 1786 (1985).

<sup>5</sup>K. Awaga, T. Sugano, and M. Kinoshita, *Chem. Phys. Lett.* **141**, 540 (1987).

<sup>6</sup>M. Kinoshita, P. Turek, M. Tamura, K. Nozawa, D. Shiomi, Y. Nakazawa, M. Isahikawa, M. Takahashi, K. Awaga, T. Inabe, and Y. Murayama, *Chem. Lett.* **1991**, 1225.

<sup>7</sup>Y. Nakazawa, M. Tamura, N. Shirakawa, D. Shiomi, M. Takahashi, M. Kinoshita, and M. Ishikawa, *Phys. Rev. B* **46**, 8906 (1992).

<sup>8</sup>M. Kinoshita, *Jpn. J. Appl. Phys., Part 1* **33**, 5718 (1994).

<sup>9</sup>R. Chiarelli, M. A. Novak, A. Rassat, and J. L. Tholence, *Nature (London)* **363**, 147 (1993).

<sup>10</sup>M. Okumura, K. Yamaguchi, M. Nakano, and W. Mori, *Chem. Phys. Lett.* **207**, 1 (1993).

<sup>11</sup>M. Okumura, W. Mori, and K. Yamaguchi, *Chem. Phys. Lett.* **219**, 36 (1994).

<sup>12</sup>K. Takeda, K. Konishi, M. Tamura, and M. Kinoshita, *Phys. Rev. B* **53**, 3374 (1996).

<sup>13</sup>K. Awaga, T. Inabe, U. Nagashima, and Y. Maruyama, *J. Chem. Soc. Chem. Commun.* **1989**, 1617; **1990**, 520.

<sup>14</sup>M. Mito, H. Nakano, T. Kawae, M. Hitaka, S. Takagi, H. Deguchi, K. Suzuki, K. Mukai, and K. Takeda, *J. Phys. Soc. Jpn.* **66**, 2147 (1997).

<sup>15</sup>Y.-I. Kim and F. Izumi, *J. Ceram. Soc. Jpn.* **102**, 401 (1994); F. Izumi, in *The Rietveld Method*, edited by R. A. Yong (Oxford University Press, Oxford, 1993), Chap. 13.

<sup>16</sup>A. Zheludev, M. Bonnet, E. Ressouche, J. Schweizer, M. Wan, and H. Wang, *J. Magn. Magn. Mater.* **135**, 147 (1994).

<sup>17</sup>K. Yamaguchi, M. Okumura, and T. Kawakami (private communication).